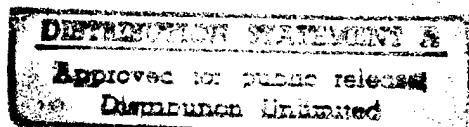


Identification of Coherent Motions using Wall Pressure Signatures

Srinath Jayasundera, Mario Casarella and Steven Russell
The Catholic University of America

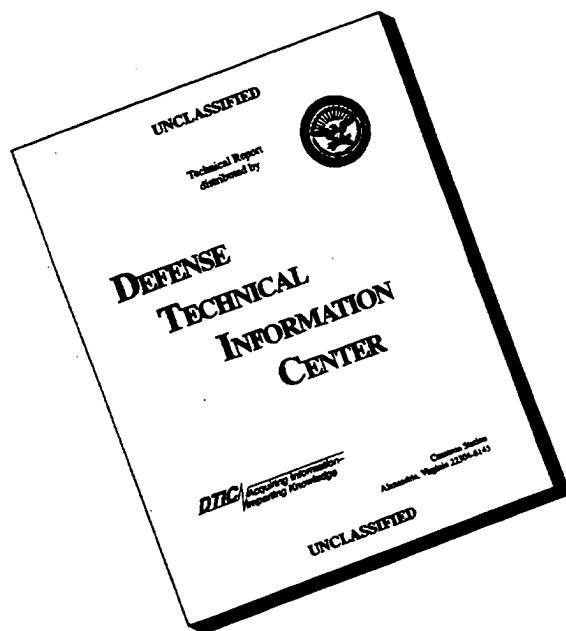
6 August 1996

19960918 036



DTIC QUALITY INSPECTED 4

DISCLAIMER NOTICE



THIS DOCUMENT IS BEST QUALITY AVAILABLE. THE COPY FURNISHED TO DTIC CONTAINED A SIGNIFICANT NUMBER OF PAGES WHICH DO NOT REPRODUCE LEGIBLY.

Identification of Coherent Motions using Wall Pressure Signatures

Srinath Jayasundera, Mario Casarella and Steven Russell
The Catholic University of America

6 August 1996

REPORT DOCUMENTATION PAGE

Form Approved
OMB No. 0704-0188

Public reporting burden for this collection of information is estimated to average 1 hour per response, including the time for reviewing instructions, searching existing data sources, gathering and maintaining the data needed, and completing and reviewing the collection of information. Send comments regarding this burden estimate or any other aspect of this collection of information, including suggestions for reducing the burden, to Washington Headquarters Service, Directorate for Information Operations and Reports, 1215 Jefferson Davis Highway, Suite 1204, Arlington, VA 22202-4302, and to the Office of Management and Budget, Paperwork Reduction Project (0704-0188), Washington, DC 20503.

| | | | | |
|--|--|---|--|--|
| 1. AGENCY USE ONLY (Leave Blank) | | 2. REPORT DATE August 6, 1996 | 3. REPORT TYPE AND DATES COVERED Progress Report 11/95 thru 11/96 | |
| 4. TITLE AND SUBTITLE Identification of Coherent Motions using Wall Pressure Signatures | | | 5. FUNDING NUMBERS N00014-94-1-0011 | |
| 6. AUTHOR(S) S. Jayasundera, M. Casarella and S. Russell | | | | |
| 7. PERFORMING ORGANIZATION NAME(S) AND ADDRESS(ES) The Catholic University of America Department of Mechanical Engineering Washington, DC 20064 | | | 8. PERFORMING ORGANIZATION REPORT NUMBER | |
| 9. SPONSORING/MONITORING AGENCY NAME(S) AND ADDRESS(ES) Office of Naval Research 800 North Quincy St. Arlington, VA 22217-5000 | | | 10. SPONSORING/MONITORING AGENCY REPORT NUMBER | |
| 11. SUPPLEMENTARY NOTES | | | | |
| 12a. DISTRIBUTION/AVAILABILITY STATEMENT Approved for public release: distribution is unlimited | | | 12b. DISTRIBUTION CODE | |
| 13. ABSTRACT (Maximum 200 words) <p style="text-align: center;">Abstract</p> <p>Large amplitude wall-pressure events observed beneath a turbulent boundary layer appear to be signatures of near-wall organized structures. Experimental investigations by the authors and their colleagues have provided strong support for this conjecture. This report contains results from new studies which attempt to identify the distinct structural features and spatial extent of the organized motions from observations of their wall pressure footprints. A database, which contains simultaneous measurements of wall-pressure, and stream-wise and wall-normal velocities at numerous locations across the boundary layer, was used in this investigation. These data are analyzed using signal processing techniques based on a trajectory mapping for the detection of coherent motions. The results show that the organized structures contain both ejection motions (accelerated events) that induce positive wall pressure events; and sweep motions (decelerated events) that induce negative wall pressure events. It is proposed that these structures collectively represent the organized motions. The present research activity is directed at the acquisition of a new database using an array of streamwise and spanwise transducers. By applying bandpass filtering techniques to the data, it is expected that the total pressure signature will become more evident.</p> | | | | |
| 14. SUBJECT TERMS Wall-pressure fluctuations, turbulent flows, organized structures, conditional sampling. | | | 15. NUMBER OF PAGES 1 | |
| | | | 16. PRICE CODE | |
| 17. SECURITY CLASSIFICATION OF REPORT UNCLASSIFIED | 18. SECURITY CLASSIFICATION OF THIS PAGE UNCLASSIFIED | 19. SECURITY CLASSIFICATION OF ABSTRACT UNCLASSIFIED | 20. LIMITATION OF ABSTRACT | |

Contents

| | | |
|-------|--|----|
| 1 | Introduction | 1 |
| 2 | Description of Signal Processing Algorithms | 4 |
| 2.1 | Trajectory Analysis Techniques (TRAT) | 4 |
| 2.1.1 | Flow Pattern Recognition and Classification | 5 |
| 2.1.2 | Ensemble-Averaged Patterns | 7 |
| 3 | Analysis of Experimental Data | 10 |
| 3.1 | Classification of coherent motions using TRAT | 10 |
| 3.1.1 | Ensemble-average shapes at fixed locations | 11 |
| 3.1.2 | Distribution of Patterns across boundary layer | 17 |
| 3.2 | Detection based on Wall-Pressure Events | 17 |
| 3.2.1 | Ensemble-averaged Results | 17 |
| 3.2.2 | Physical features of flow structures | 22 |
| 4 | Concluding Remarks and Future Work | 27 |
| | Acknowledgements | 28 |
| | References | 29 |

Abstract

Large amplitude wall-pressure events observed beneath a turbulent boundary layer appear to be signatures of near-wall organized structures. Experimental investigations by the authors and their colleagues have provided strong support for this conjecture. This report contains results from new studies which attempt to identify the distinct structural features and spatial extent of the organized motions from observations of their wall pressure footprints. The database of Kammeyer [1], which contains simultaneous measurements of wall- pressure, and streamwise and wall-normal velocities at numerous locations across the boundary layer, was used in this investigation. These data are analyzed using signal processing techniques based on a trajectory mapping for the detection of coherent motions as proposed by Nagano and Tagawa [4]. The results show that the organized structures contain both ejection motions (accelerated events) that induce positive wall pressure events; and sweep motions (decelerated events) that induce negative wall pressure events. It is proposed that these structures collectively represent the organized motions. The present research activity is directed at the acquisition of a new database using an array of streamwise and spanwise transducers. By applying bandpass filtering techniques to the data, it is expected that the total pressure signature will become more evident.

Chapter 1

Introduction

Large amplitude wall-pressure events observed beneath a turbulent boundary layer appear to be signatures of intermittent organized motions within the turbulent flow. Experimental studies were made by Kammeyer [1] investigating this relationship. Simultaneous measurements of the fluctuating wall-pressure, and streamwise and wall-normal velocities were obtained. These measurements were acquired at numerous locations across the boundary layers. A filtering technique based on the wavelet transform was developed to isolate the near-wall burst motions from the outer-layer disturbances. Correlation and conditional sampling were performed based on the detection of cluster patterns of wall-pressure and turbulence-producing flow events.

The results confirm that patterns of high frequency large-amplitude wall-pressure events are footprints of the active (turbulence-producing) motions. The results of near wall flow field mappings show at least two vortices, one ahead and above the other, that induce the ejection/sweep pattern and a concomitant positive wall-pressure peak aligned with the ejection. The resulting shear front is inclined downstream and extends to the log-law region. This picture is consistent with models proposed by several investigators.

The signal processing techniques developed in the research investigation were successful in isolating the clusters of peak events along the time records. A Peak Detection (LWPD) algorithm was created for the detection of groupings of both the burst events within the flow and the surface pressure signatures of these organized structures. Correlation and conditional sampling methods were used to show that cluster patterns of bursts and wall-pressure events appear to be aligned, and that positive wall-pressure peaks appear to

identify the Q2 (ejection) events within the burst patterns.

In addition, these results support the conjecture that combinations of Q2 and Q4 burst events are features of organized structures identified by the large-amplitude wall-pressure signatures (figure 1). Using detection theory for classification, Penafiel [2] recently showed that paired combinations of Q2 & Q4 events dominate the cluster pattern of burst events. The identification of paired patterns had also been confirmed by Wilczynski [3].

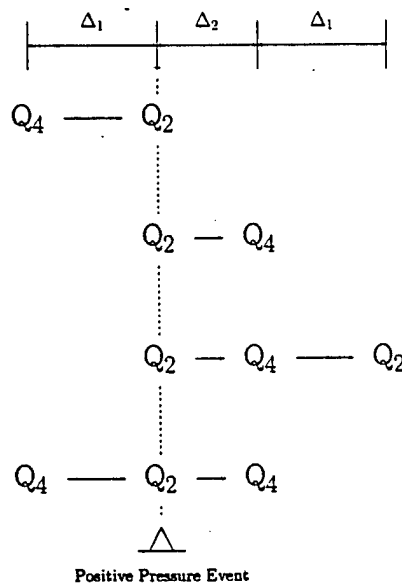


Fig. 1. Alignment of Q2 and Q4 Patterns (from reference 5)
 $(\Delta_1 \approx 14t^+$ units, $\Delta_2 \approx 11t^+$ units)

This study is a continuation of previous investigations on the identification of coherent motion by means of their wall pressure footprint. The raw database on equilibrium flows established by Kammeyer [1] is analyzed us-

ing signal processing techniques based on a trajectory-based algorithm for detection of coherent motions. This trajectory analysis technique was developed by Nagano and Tagawa [4]. The correspondence between wall pressure events and cluster patterns of coherent motion will be reexamined. This report presents the preliminary findings from these computations.

Chapter 2

Description of Signal Processing Algorithms

2.1 Trajectory Analysis Techniques (TRAT)

Nagano *et. al.* [4] investigated the relationship between coherent motions and heat transfer in pipe flow. They developed a new methodology for detecting and extracting coherent motions from time-series data of turbulence. Traditional detection schemes for coherent motion such as VITA methods or quadrant splitting techniques have been used in the past by many investigators, including the authors, with limited success in pattern recognition. The method proposed by Nagano *et. al.* [4] was an attempt to improve on these traditional algorithms.

A trajectory analysis technique was formulated based on the premise that the existence of coherent motions requires regularity in the trajectory of the motion projected on the (u,v) plane. This premise has its foundation in the requirement for continuity of fluid motions. They observed several basic trajectory patterns that are consistent with Q2/Q4 and Q4/Q2 patterns observed by Casarella, Penafiel and Kammeyer [5]. In contrast to Casarella *et. al.* [5] the technique preserves the phase information between the fluctuating components u and v by retaining the quadrant transitions Q_i between Q2 and Q4 events (figure 2). This method of classification (referred to as TRAT) extract those patterns that contribute to turbulent production. Retaining the trajectory in each of the three quadrants during the motion is

central to the pattern recognition of organized motions.

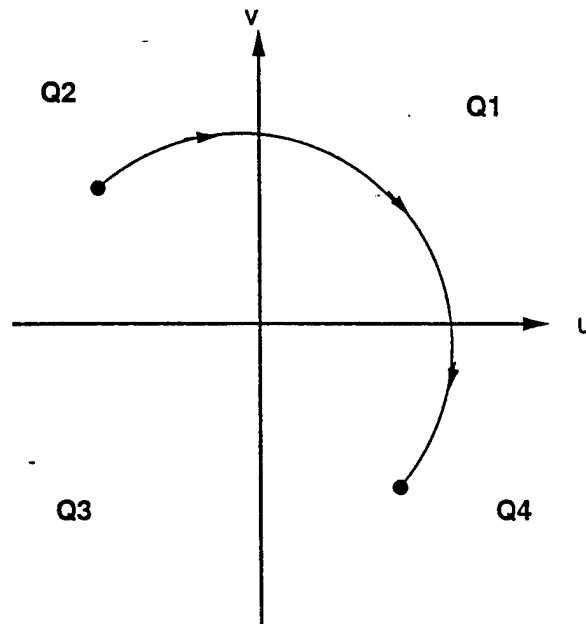


Fig. 2. Trajectory Pattern Q2-Q1-Q4 (accelerated motion)

2.1.1 Flow Pattern Recognition and Classification

The TRAT technique requires the concurrent time records on $u(t)$ and $v(t)$ as input to the algorithm. It consists of the following steps:

1. Using fluctuating velocities u and v , the total time record of fluid motions is classified as $Q_i(t)$; $i=1,2,3,4$ where i denotes the quadrant in the (u,v) plane.
2. Obtain a time-series of quadrant sequences $Q_i(1), Q_i(2), Q_i(3), \dots, Q_i(j) \dots$ where i denotes the classification and j is an integer index which in-

creases by 1 whenever a trajectory crosses a boundary of a quadrant of the (u,v) plane.

3. The resulting time series of quadrants is decomposed and classified into a total of 36 patterns which are permutations and combinations of three quadrants; $Q_{i_1} - Q_{i_2} - Q_{i_3}$, where Q_{i_2} is referred to as the **transition event**. In the process, if $|\bar{u}v(j-1)| \leq Hu_{rms}v_{rms}$, $|uv(j)| \leq Hu_{rms}v_{rms}$, $|uv(j+1)| \leq Hu_{rms}v_{rms}$ are satisfied simultaneously, the pattern is discarded¹.

The algorithm was fully tested with both random data and real data. For example, the algorithm was tested using u and v time records from different test runs as the random data test. The results were consistent with white noise data.

The TRAT classification technique can be modified and used in conjunction with other detection algorithms such as the VITA method or peak detection scheme. In these cases, the time locations of event occurrence are prescribed by the detection scheme, and classification of the triplet pattern is only made at these prescribed locations. This essentially allows for pattern recognition at the location of recognized events. Nagano *et. al.* [4] used the VITA technique for event detection and the TRAT algorithm for classification. They showed that the traditional VITA technique with the slope criteria has shortcoming in detecting flow structures associated with heat transfer mechanisms. This is attributed to the distinction between Q2/Q4 flow patterns with different transition events.

In this investigation, several combinations of detection and classification schemes were examined using $H = 1.07$. The pure TRAT technique and VITA plus TRAT methods were first applied to the database of Kammeyer. These findings were compared to the results of Nagano *et. al.* [4]. Subsequently, both LWPD and peak pressure detection algorithms were used for event detection on the wall pressure time records and the TRAT classification algorithm applied to the uv data. This was done using a variety of filtered schemes. Only the results for the pure TRAT and peak pressure detection plus TRAT on unfiltered data will be presented in this report.

¹It should be noted that Nagano *et. al.* [4] also introduces a threshold value 'h' on $|u|$ and $|v|$ that must be satisfied for a pattern to be accepted. Test runs indicated that this threshold was not needed with our database.

After extensive real data testing, only 16 patterns were found to be relevant to organized motions, instead of 36 patterns originally proposed by Nagano *et. al.* [4]. These 16 patterns were divided into four groups as shown in figure 3. The four groups represent counter-clockwise rotational motion, clockwise rotational motion, counter-clockwise oscillations and clockwise oscillations, respectively.

Groups I and II contain the patterns identified by Kammeyer [1, 5] as the dominant near-wall structures associated with turbulent production. These are the Q2 and Q4 combinations labeled in figure 3. It should be noted that these four basic flow structures:

| | |
|----------|----------|
| Q2-Q1-Q4 | Q4-Q1-Q2 |
| Q2-Q3-Q4 | Q4-Q3-Q2 |

are also the key patterns identified by Nagano *et. al.* [4]. The results to be presented will support these findings and show that, in fact, only groups I and II are of practical importance.

2.1.2 Ensemble-Averaged Patterns

The 36 distinct patterns were ensembled averaged for all patterns observed over the time record. Nagano *et. al.* [4] performed the averaging by adjusting the temporal duration of each event to the mean duration of the respective Q_i motions. The results to be presented did not require this modification. However, the events were aligned before averaging with the axes crossing between Q_i motions. A bias towards u changing from negative to positive values ($Q3 \rightarrow Q4$ or $Q2 \rightarrow Q1$) representing accelerating motion; or positive to negative values ($Q4 \rightarrow Q3$ or $Q1 \rightarrow Q2$) representing decelerating motions, was made in selecting which of the two axes crossings to use for alignment.

It will be argued that accelerated motions characterize ejections and consist of Q2/Q4 patterns

| | | | | | |
|----|---|----|---|----|---|
| Q2 | - | Q3 | - | Q4 | |
| Q3 | - | Q4 | - | Q1 | * |
| Q2 | - | Q1 | - | Q4 | |
| Q3 | - | Q2 | - | Q1 | * |

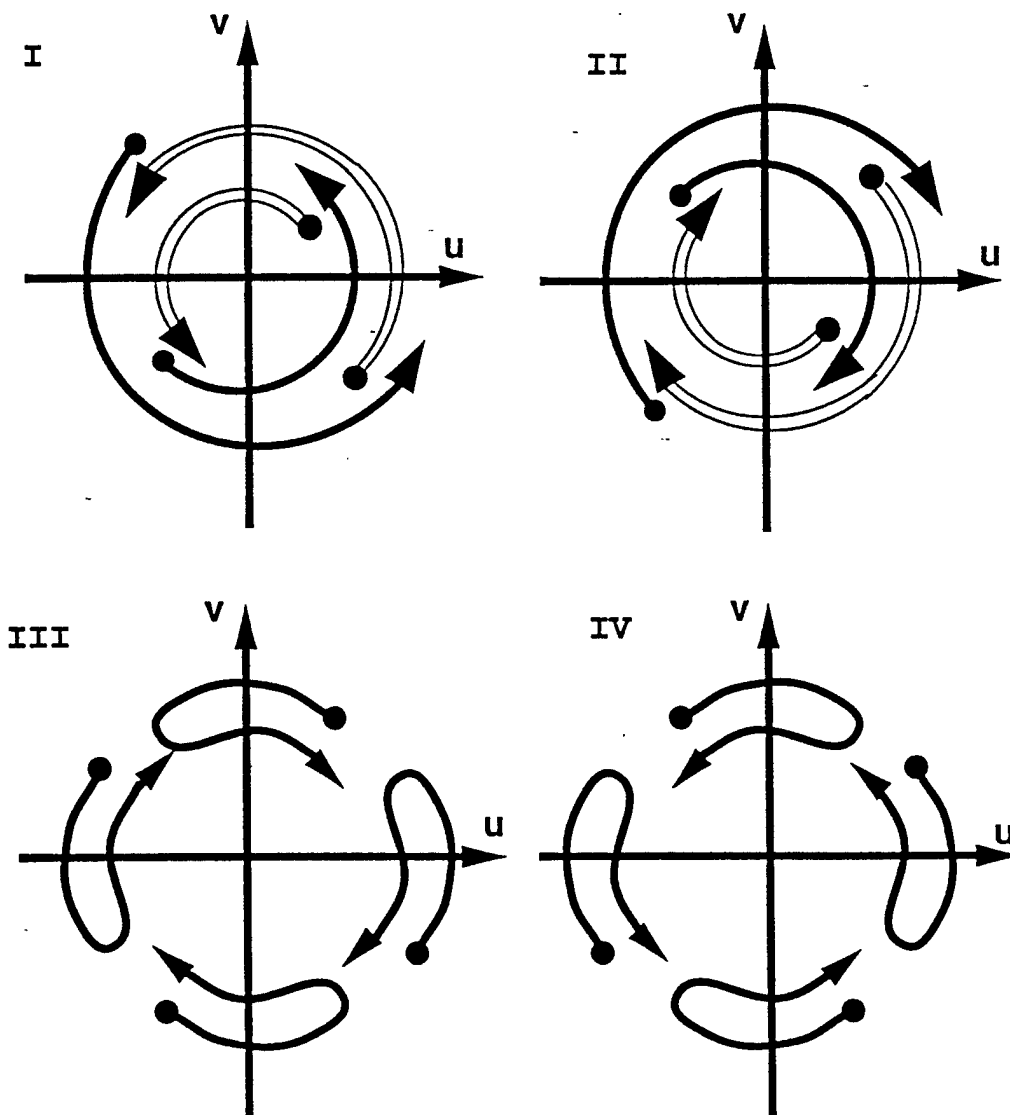


Fig. 3. Classification of major patterns to 4 groups; Group I: Q1-Q2-Q3, Q2-Q3-Q4, Q3-Q4-Q1, Q4-Q1-Q2; Group II: Q1-Q4-Q3, Q2-Q1-Q4, Q3-Q2-Q1, Q4-Q3-Q2; Group III: Q1-Q2-Q1, Q2-Q3-Q2, Q3-Q4-Q3, Q4-Q1-Q4; Group IV: Q1-Q4-Q1, Q2-Q1-Q2, Q3-Q2-Q3, Q4-Q3-Q4. Solid lines in Groups I and II correspond to accelerated motions and induce positive pressure events while hollow lines corresponds to decelerated motions and induce negative pressure events.

These structures produce **positive wall peak pressure events**.

It will also be argued that deceleration motions characterize sweeps and consists of Q4/Q2 patterns

Q4 - Q3 - Q2
Q1 - Q4 - Q3 *
Q4 - Q1 - Q2
Q1 - Q2 - Q3 *

These motions produced **negative peak pressure events**.

These flow patterns are contained exclusively in Groups I and II (figure 3). It is most likely that the shortcomings in the classification algorithm have mis-aligned the * patterns and that these essentially are contained within the four basic Q2/Q4 and Q4/Q2 patterns. The data to be presented partially support this hypothesis.

Chapter 3

Analysis of Experimental Data

3.1 Classification of coherent motions using TRAT

The TRAT method in its most general form allows for the classification of 36 patterns of fluid motion. The algorithm was applied to the time records of $u(t)$ and $v(t)$ at 19 location across the boundary layer. The classification of distinct patterns were made at each of these locations. The results at the near-wall location on the frequency of occurrence of each pattern were, generally speaking, consistent with Nagano *et. al.* [4]. However we disagree on several features including their quantitative data comparing pseudo-turbulence with actual wall turbulence; and their findings and interpretations of the sub-patterns.

It should also be noted that the algorithm has shortcomings which must be recognized during interpretations of the results. The grouping are based on permutations and combinations of (only) three quadrants along the time records. This permits the inclusion of overlapping patterns. Consequently the distribution on the frequency of occurrence of events can be misleading. Furthermore, the phase-jitter between u and v can affect the classification.

The results to be presented in this section will focus only on the 16 patterns identified by the four groups. These patterns appear to be the most meaningful for characterizing the organized motions. This will be confirmed with the mapping of the flow patterns. Table 1 list the number of events found in each of these groups at the $y^+ = 25$ location. The subtotal of

events for these four groups (13,264 events) represents approximately 70% of the total number of events classified by TRAT.

| Group | Number of Events |
|-------|------------------|
| I | 3274 |
| II | 3515 |
| III | 3316 |
| IV | 3159 |
| Total | 13,264 |

Table I

3.1.1 Ensemble-average shapes at fixed locations

The shortcomings previously discussed on the TRAT algorithm were partially overcome by aligning the individual events at the axis crossing for the transition between Q_i events prior to ensemble averaging. It is well-established from the VITA + slope detection method that the accelerated and decelerated changes in streamwise velocity u correlate with positive and negative wall pressure events, respectively [8]. Therefore the axis crossings between positive slopes (Q3-Q4 or Q2-Q1) and negative slopes (Q4-Q3 or Q1-Q2) on the u velocity were selected for alignment locations in groups I and II.

Figures 4 thru 7 show the ensemble-averaged results on flow structures at the near-wall location $y^+ = 25$ for groups I, II, III and IV, respectively. The 4 patterns contained in each figure represent the patterns for the respective group. The ensemble averages of the concurrent wall pressure events that coincide with the respective organized motions are also included. These results on wall pressure are very sensitive to the phase-jitter between turbulent events and their wall pressure signatures (Phase-jitter correction are often applied prior to ensemble-averaging).

The results confirm that Groups I and II produce both positive and negative wall pressure events. Individual flow structures within each group include accelerated motions (ejections) causing positive events; and decelerated motion (sweeps) causing negative pressure events. For these results, the phase relationships between the location of the peak pressure and the u -axis crossing are bounded by the viscous time scale, $\Delta t^+ \leq 10$.

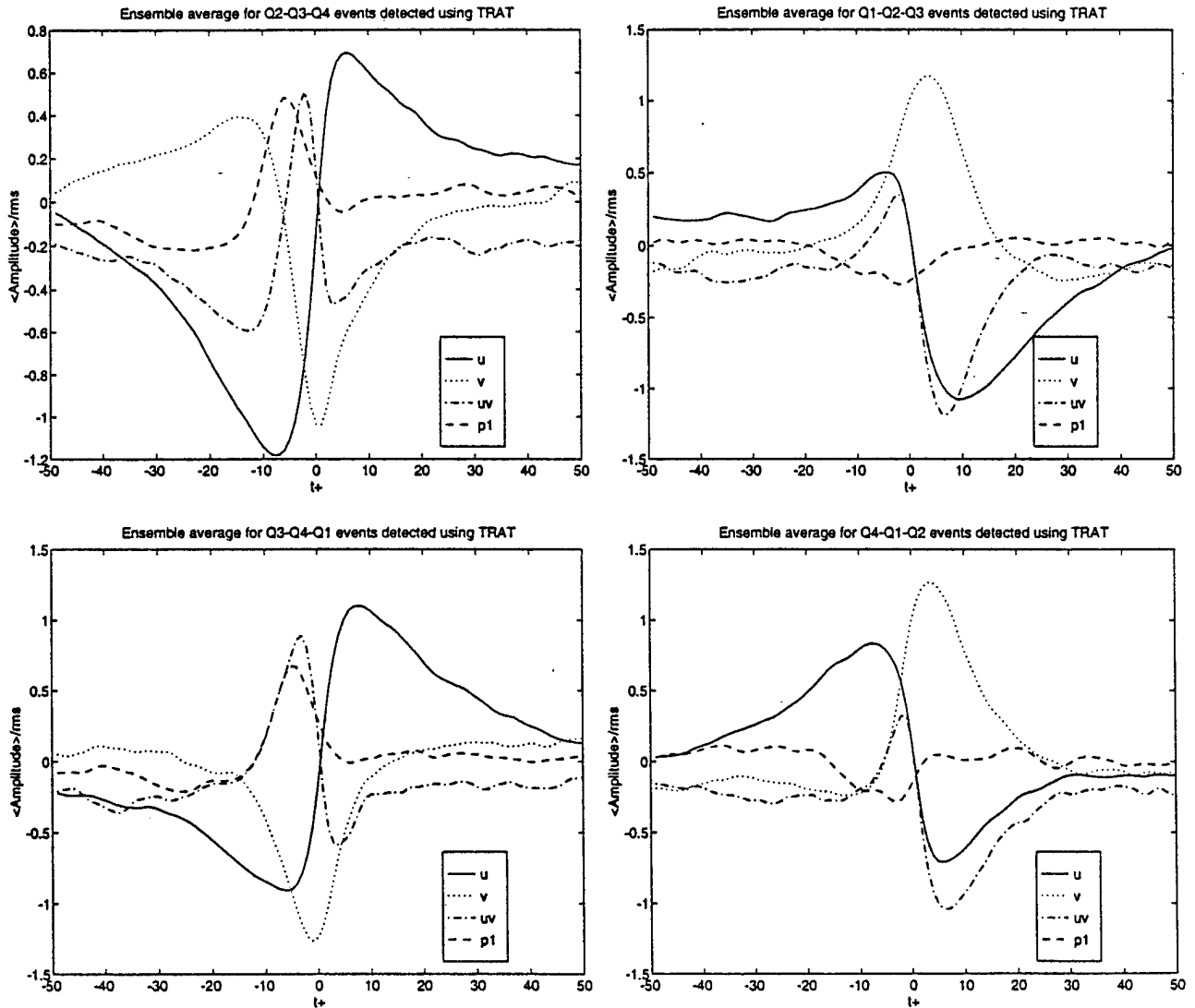


Fig. 4. Ensemble average for Group I

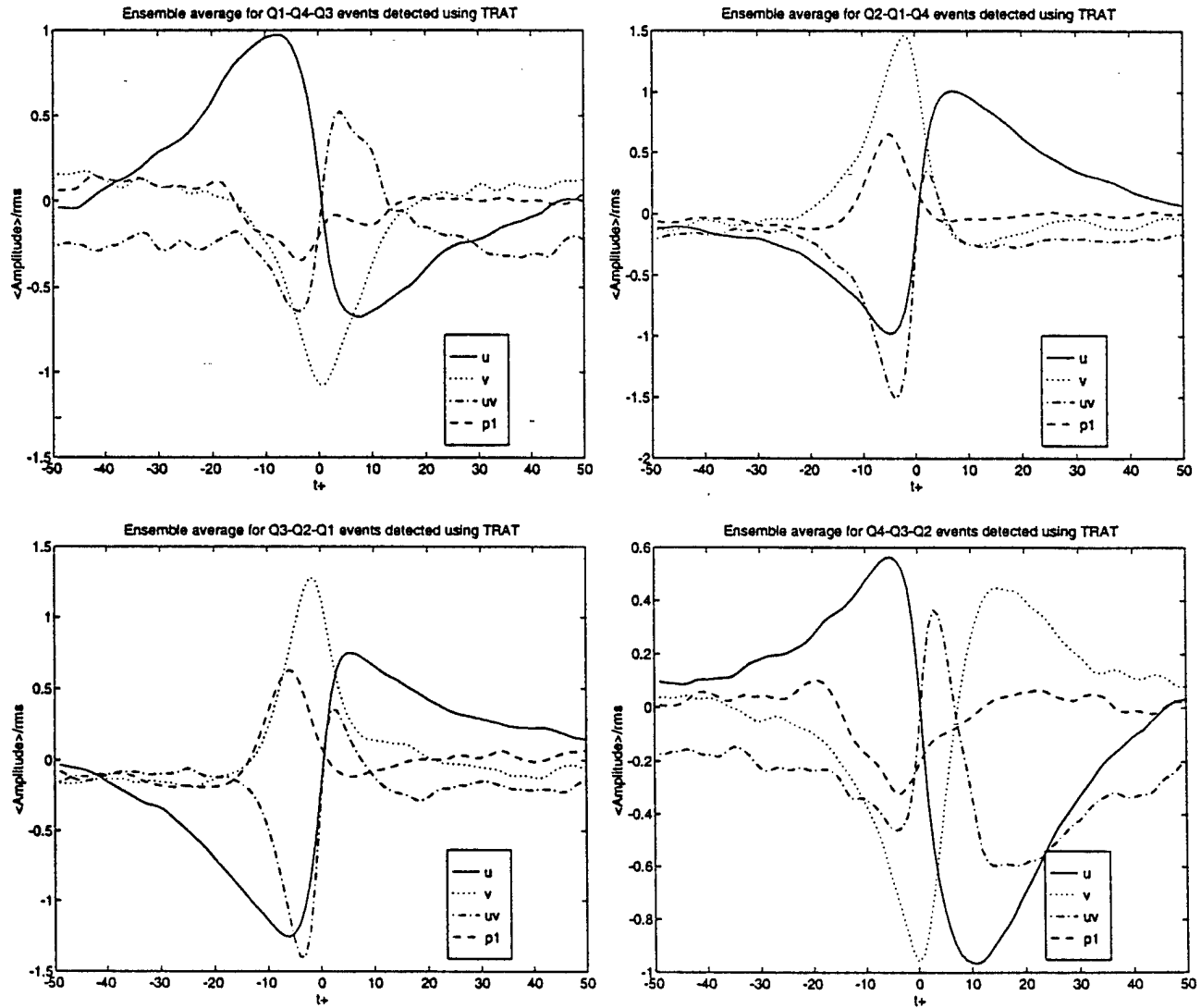


Fig. 5. Ensemble average for Group II

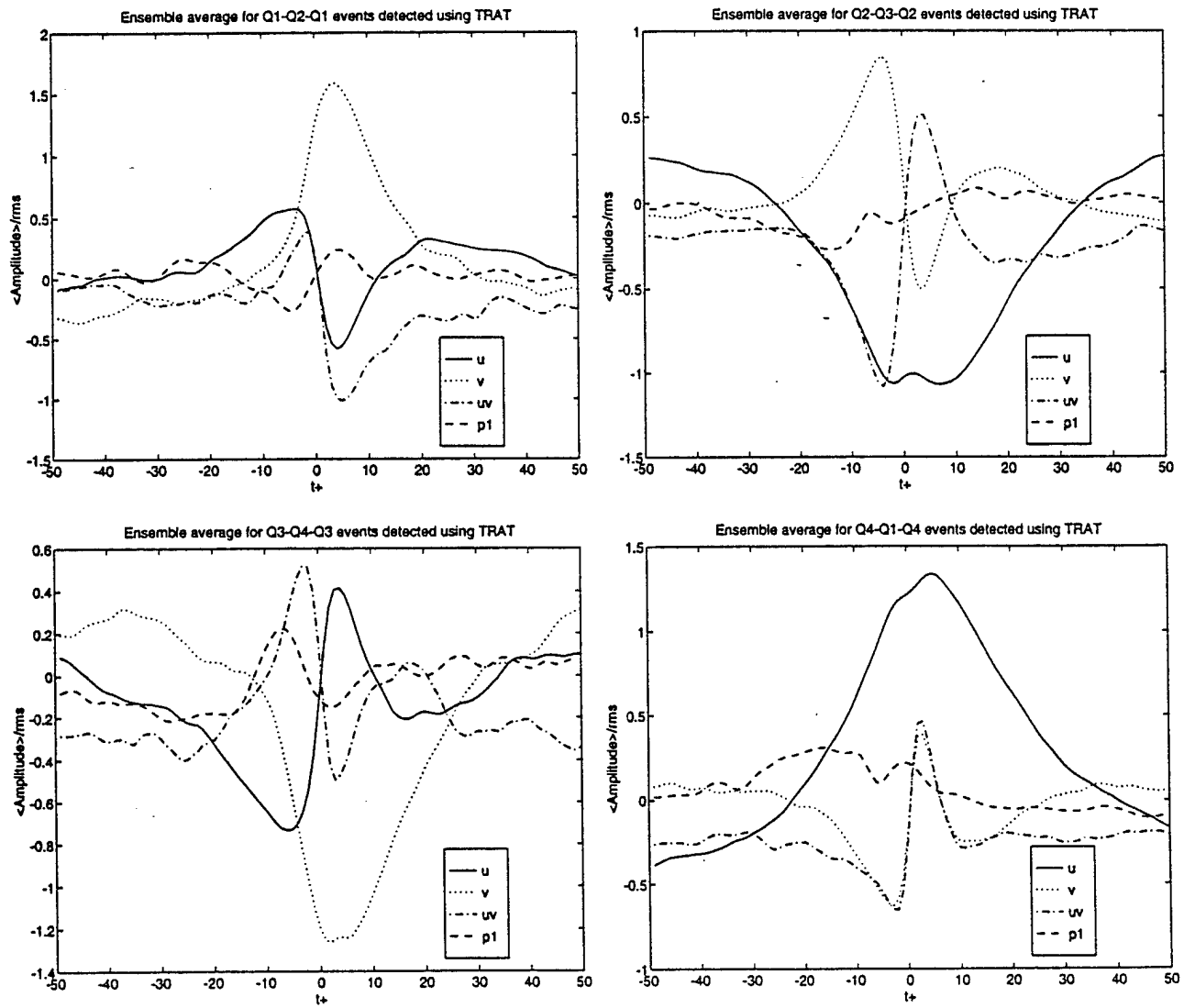


Fig. 6. Ensemble average for Group III

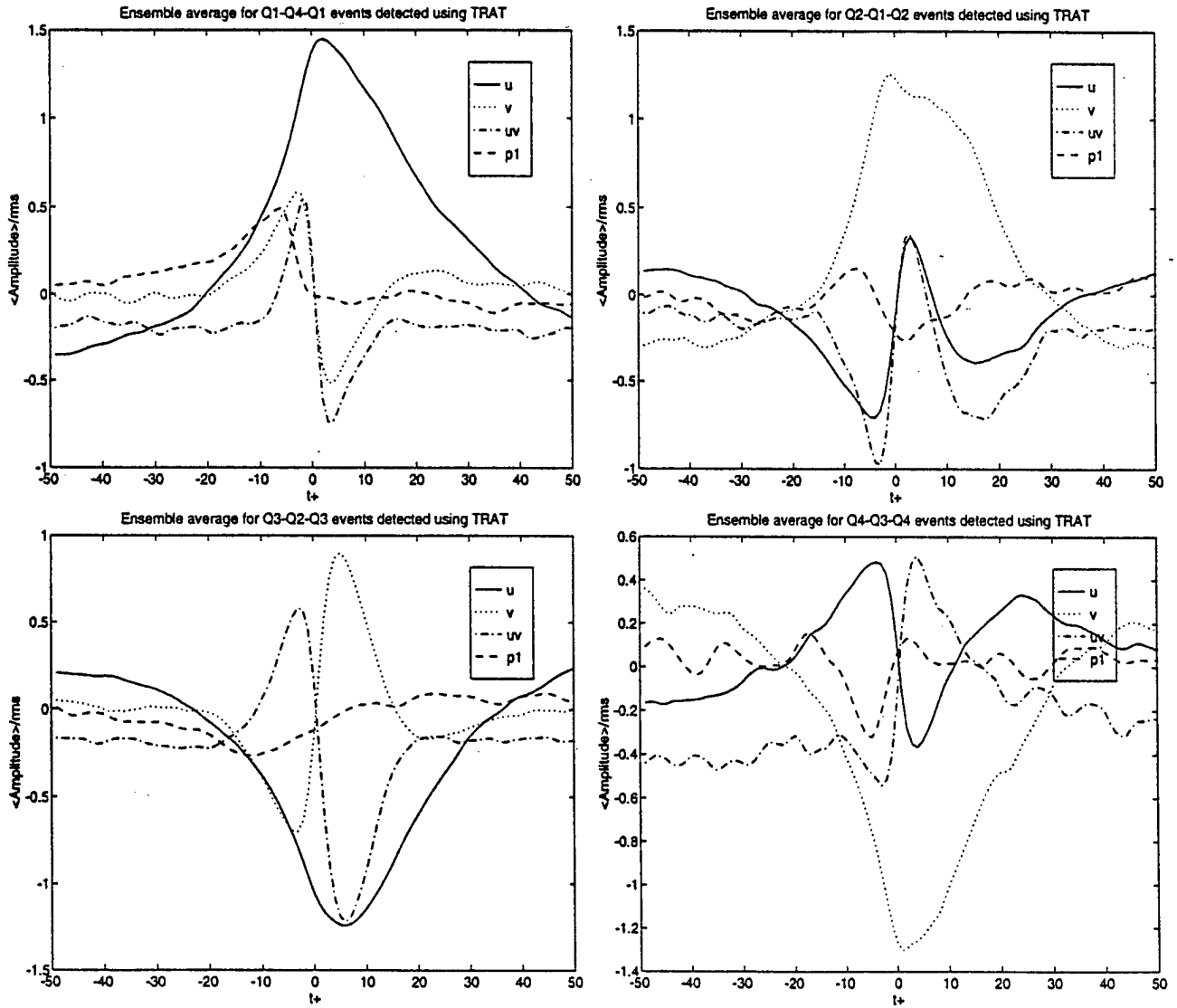


Fig. 7. Ensemble average for Group IV

In examining the relationship between coherent motion and passive scalar heat transfer in pipe flows, Nagano *et. al.* [4] concluded that the distinctions between accelerated motions labeled Q2-Q3-Q4 and Q2-Q1-Q4; as well as between decelerated motions labeled Q4-Q3-Q2 and Q4-Q1-Q2 were important. This was not the case in our results when observing the wall pressure footprint of these structures. The results in figures 4 and 5 show that pressure signatures of both acceleration motion patterns were similar despite opposite signs for the v component of the perturbations. Similar pressure patterns were observed on the decelerated motions. It is not clear what the distinct role of the transition-events Q_i within the patterns is on organized motions. What is clear is that the flowfield maps of the two patterns are quite different.

The conjecture made earlier in the report that the ejection motions Q3-Q2-Q1 and Q3-Q4-Q1 are, in fact, misaligned Q2-Q1-Q4 and Q2-Q3-Q4 respectively, is supported by the data shown in figures 4 and 5. Support for the sweep motions Q1-Q4-Q3 and Q1-Q2-Q3 being actually misaligned Q4-Q3-Q2 and Q4-Q1-Q2 patterns respectively is also evident in the data.

In summary, the data supports the hypothesis that four basic types of flow structures exist:

Ejection motions (positive wall pressure events)

- Q2 - Q1 - Q4
- Q2 - Q3 - Q4

Sweep motions (negative wall pressure events)

- Q4 - Q1 - Q2
- Q4 - Q3 - Q2

It appears that these structures collectively represent the organized motion. Therefore, the total footprint of the turbulent structure contains both positive and negative pressure peaks.

Nagano *et. al.* [4] attempted to assess the overall features of the turbulent structure based on the ensemble-averaged patterns observed at near-wall location $y^+ = 18.5$. They examined the correspondence between TRAT results and flow visualization data of Bogard and Tiederman [6]. Bogard and Tiederman proposed that ejections are the primary motions in organized

structures and consist of three parts; leading edge, middle and trailing edge. Nagano *et. al.* [4] suggested that these motions correspond to Q4-Q3-Q2, Q3-Q2-Q3 and Q2-Q3-Q4, respectively. Their results at $y^+ = 18.5$ compare favorably with flow visualization results at $y^+ = 15$. Since these data were restricted to the buffer layer $y^+ < 30$ and are observed at only a single y location, the conjecture can be questioned.

3.1.2 Distribution of Patterns across boundary layer

The 16 flow patterns contained in Groups I, II, III and IV were classified by the TRAT technique at each of the 19 locations across the boundary layer. The percentage of events for each classification were computed at each of these locations. The collection of events at each location were then ensemble-averaged.

The results to be presented will focus only on the four basic patterns of ejection and sweep motions previously discussed. Figures 8a and 8b show the percentage of events, fractional contribution to \overline{uv} and percentage contribution to P_{rms} at each location across the boundary layer. It appears that these flow structures dominate the near wall region, but no clear perception on the spatial extent of these organized structures can be deduced from these findings.

The results for the ensemble-averaged patterns at locations $y^+ = 50, 94, 173, 214, 303$ and 540 were more enlightening as to the spatial extent of the organized structure. The ejection motions associated with positive pressure events were observed for $y^+ \leq 214$ while the sweep motions extended slightly further to $y^+ \leq 303$. This is consistent with near-wall ejections and outer layer sweep motions.

3.2 Detection based on Wall-Pressure Events

3.2.1 Ensemble-averaged Results

Kammeyer [1] had shown that by conditional sampling on wall pressure events and ensemble-averaging the coincident u and v components at each location in the boundary layer, burst/sweep events can be detected.

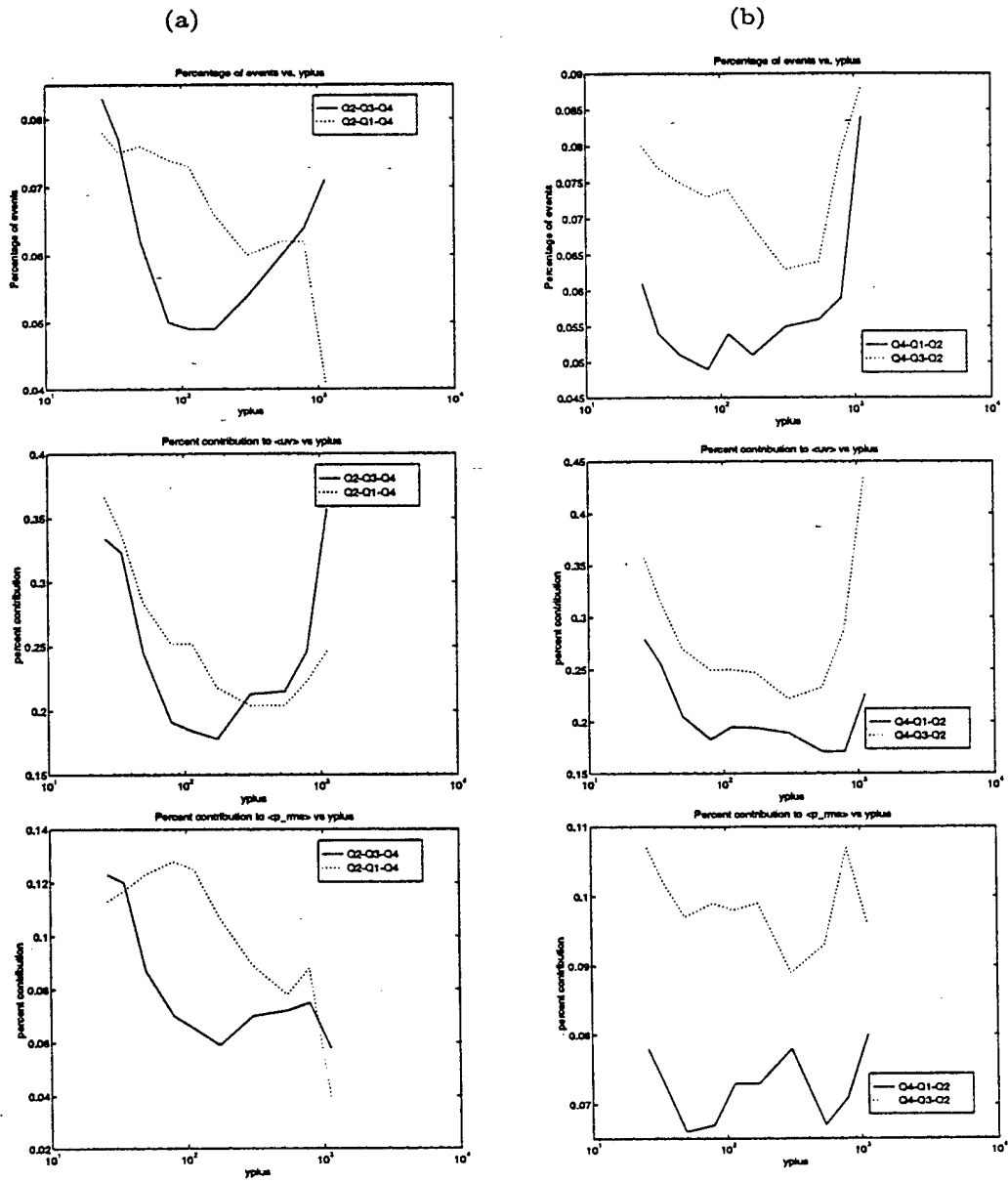


Fig. 8. Percentage of events (top), percentage contribution to $\langle uv \rangle$ (middle) and percentage contribution to $\langle prms \rangle$ (bottom)

An algorithm was written that allowed the detection of positive and negative peak wall pressure events along the time records at these locations. The TRAT classification scheme was then applied to the concurrent $u(t)$ and $v(t)$ time records. The flow coincident with detected wall pressure events are observed. (This is the reverse situation to that discussed in section 3.1.1 and illustrated in figures 4 thru 7). The software was tested with fabricated data to validate the algorithm. Pressure data obtained at the y_{i+1} location were used to obtain peak values and these locations were used to classify $u(t)$ and $v(t)$ at the y_i location. For this artificial dataset, the results were consistent with white noise.

Figure 9 shows the results on real data for the detection of Q2/Q4 flow structures based on positive peaks in wall pressure events ($p_w \geq 2p_{rms}$). The ensemble-averages of the four flow patterns associated with the ejection process at location $y^+ = 25$ are shown. Clearly, the peak pressures align with the accelerated structure. This is consistent with the results presented in figures 4 and 5 using pure TRAT classification where positive wall pressure events were observed as signatures of these classified patterns. Thus, it has been shown that a bidirectional relationship exists between positive peak pressures and Q2/Q4 ejection patterns.

It should be noted that these results are not new nor surprising since the conventional VITA + slope method has produced similar results. However, it validates the merits of using the traditional VITA method. This popular method has significant advantages since it requires only the u component of velocity for detection.

Figure 10 shows the results of detection of Q4/Q2 flow structures based on negative peaks in wall pressure events ($p_w \leq -2p_{rms}$). The ensemble-averaged patterns associated with the sweep process at locations $y^+ = 25$ are shown. Again, the negative pressure peaks align with decelerated structures.

It should also be noted that for the results presented in figures 9 and 10, the phase alignments of the location for the peak pressure with the u -axis crossing have some scatter but are reasonably well bounded similar to the data presented in figures 4 and 5. However, the phase alignments of the positive and negative pressure peaks with the u -axis crossings shown in figures 9 and 10 respectively, are not consistent in showing definitive trend for the respective cases. Most algorithms will force the alignment of the axis crossing with the local peak and call this a phase-jitter correction, but this can produce misleading results.

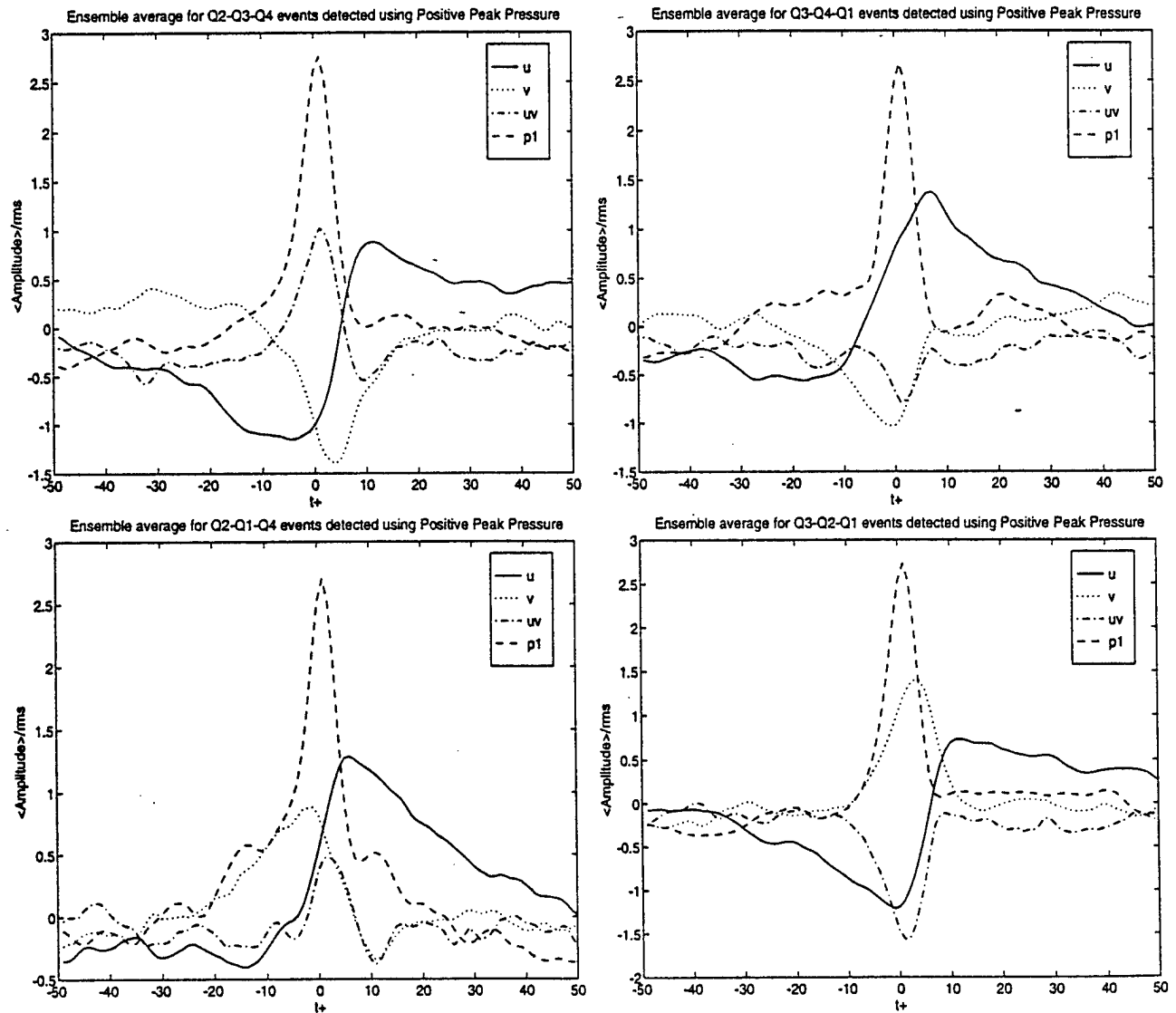


Fig. 9. Ensemble average for detection based on positive wall pressure events

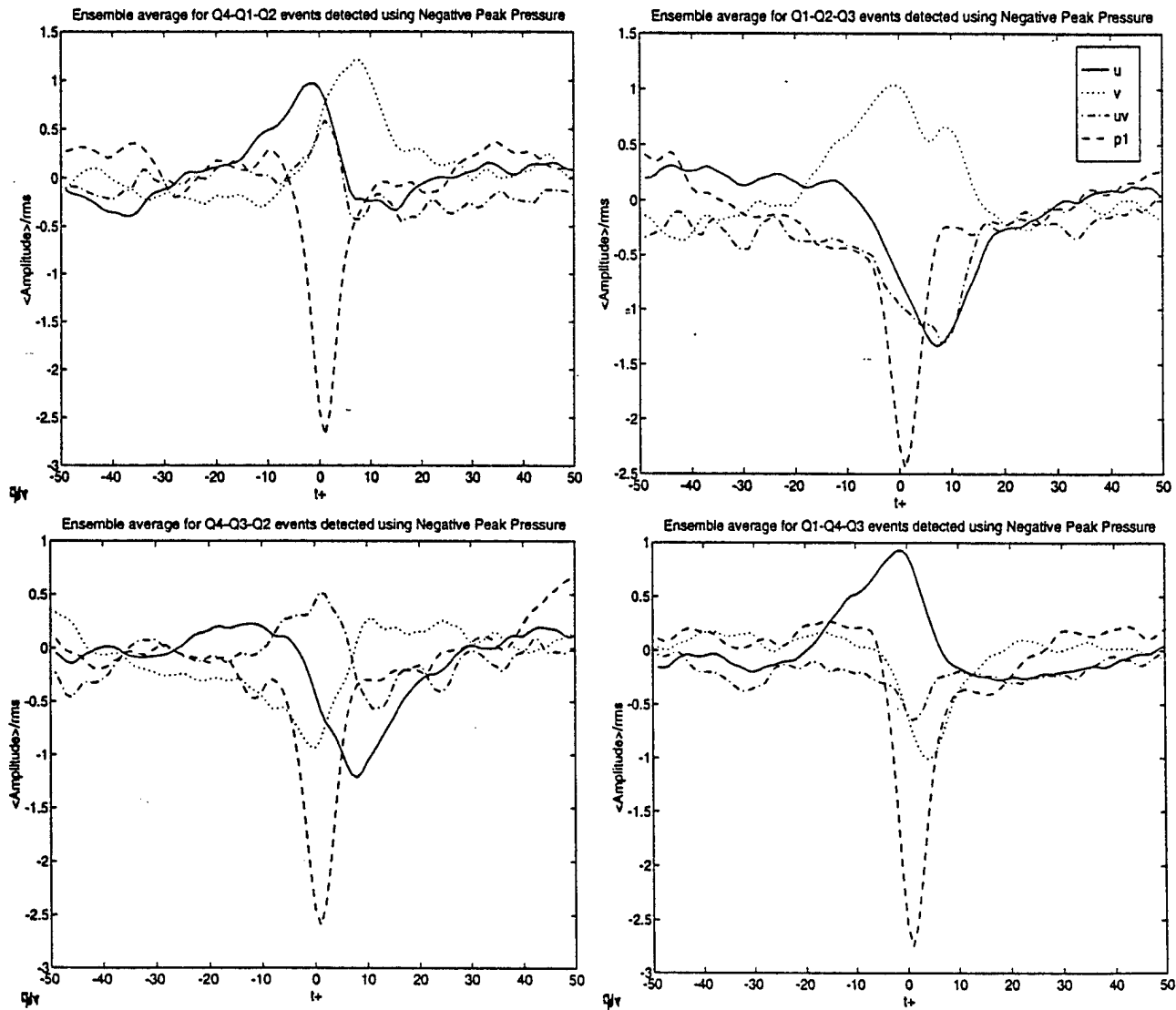


Fig. 9. Ensemble average for detection based on positive wall pressure events

3.2.2 Physical features of flow structures

Kammeyer [1] used wall pressure detection and formulated a composite picture of the observed flowfield structure. He mapped the velocity field obtained from the ensemble-averaged data at each y location. The data were mapped spatially by the transformation

$$X_{u,v} = -U(y).t$$

$$X_p = -U_c.t$$

where U_c is the convection velocity computed from wall pressure data obtained from multiple streamwise transducers. In this investigation, these mappings were done for the ensemble-averaged TRAT classification patterns using both positive peak pressure detection ($p_w \geq 2p_{rms}$) and negative peak pressure detection ($p_w \leq -2p_{rms}$).

Figures 11 a,b,c show the results for positive peak detection on wall pressure. Three different cases of ensemble-averaging of the flow structures are shown; 36 patterns (all events), 16 patterns (Groups I thru IV) and 8 patterns (Groups I and II). No appreciable differences were observed between the three cases. This supports the conjecture that the flow structure in groups I and II, representing the ejection/ sweep motions, dominate the organized motions. It should also be noted that since positive peaks in wall pressure were exclusively detected, then the ensemble-average results display structure primarily associated with near-wall ejections.

Figure 12 displays the results for negative peak detection on wall pressure. Again, three different cases of ensemble-averages of the flow structure are shown with no significant differences in the results. This further supports the dominance of flow structures in Groups I and II. In this case, negative peaks in pressure were detected and the ensemble-averaged results reflect the outer-layer sweep motion.

The conclusions from the results shown in figures 11 and 12 are that the positive peak pressure events and negative peak pressure events track different aspects of the organized motion. These results, along with previous results shown in figures 9 and 10, show that the positive peaks track the accelerated motion associated with ejection process; and negative peaks track the decelerated motion associated with the sweep motion.

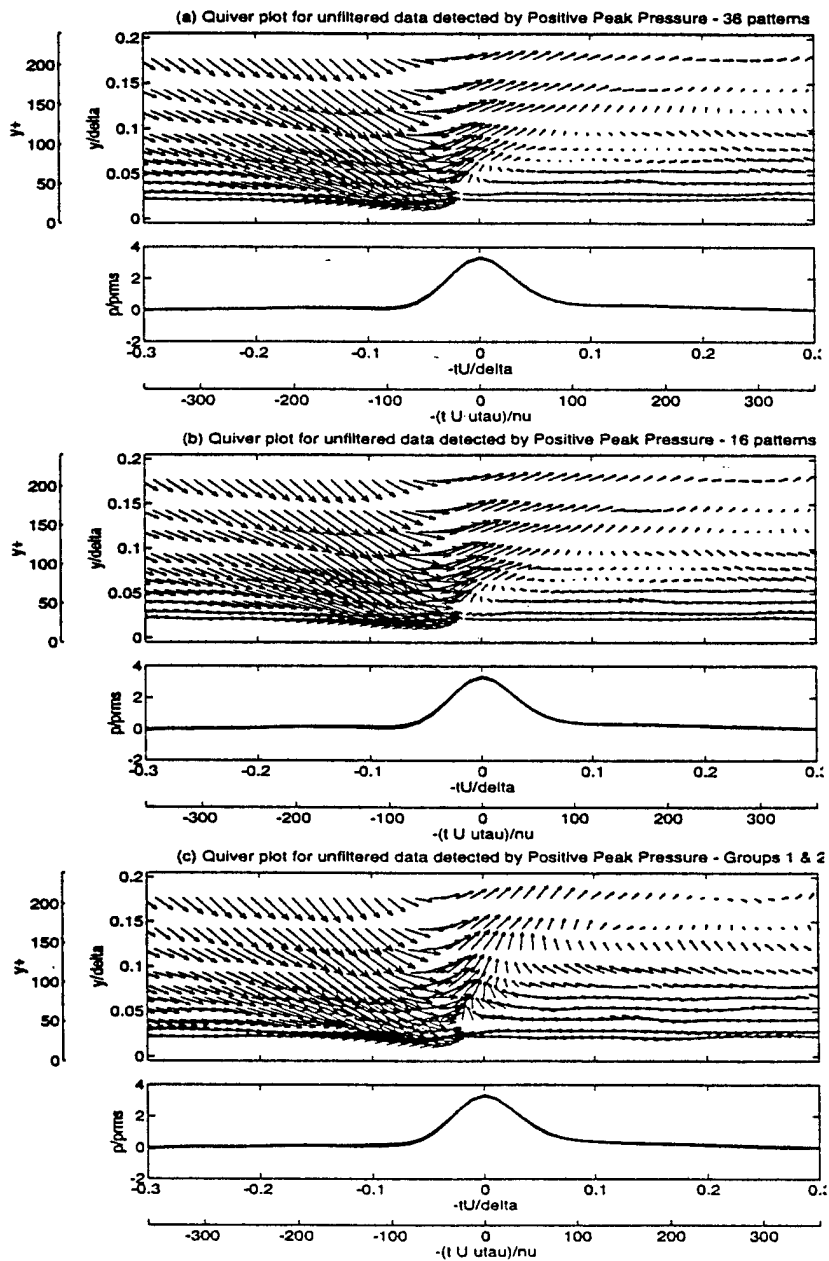


Fig. 11. Quiver plots resulting in positive peak detection

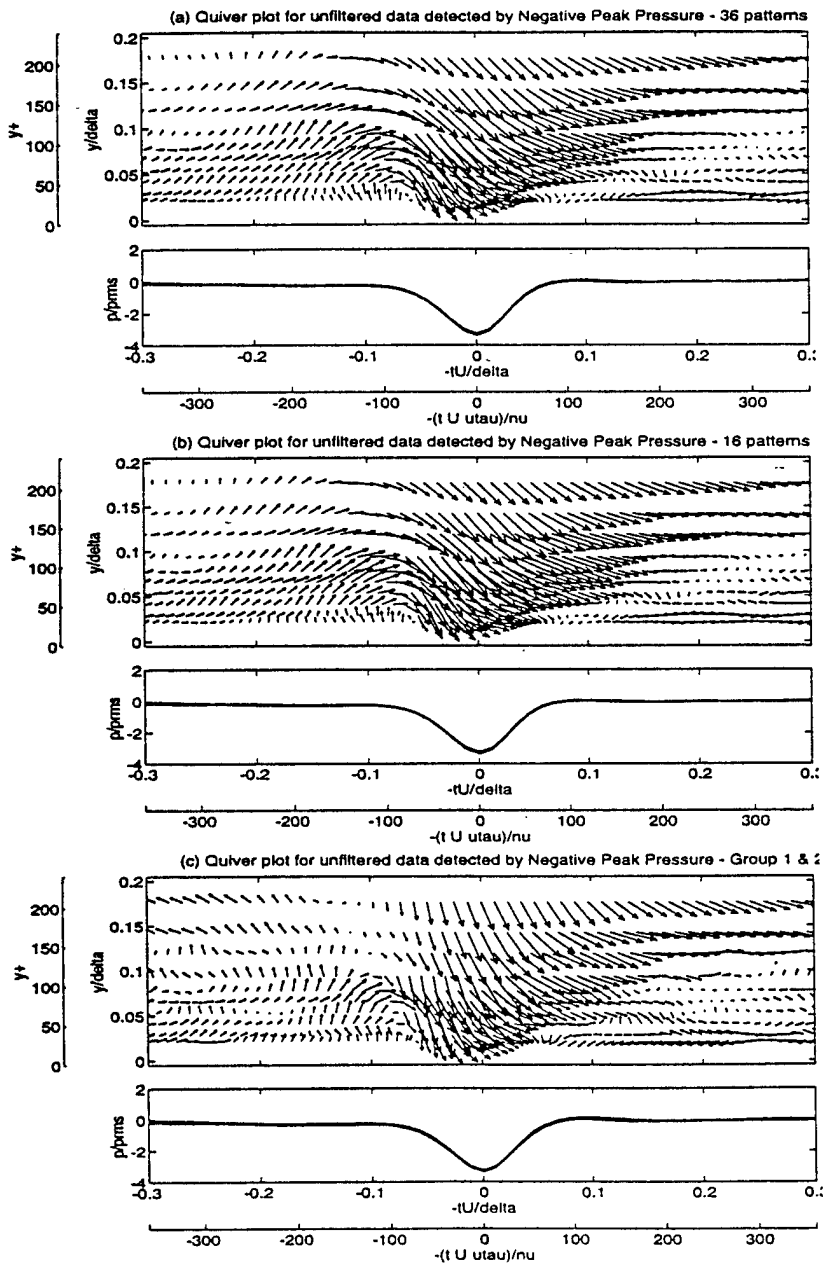


Fig. 12. Quiver plots resulting in negative peak detection

It is tempting to further examine the four patterns exclusively associated with ejections and the 4 patterns associated with sweeps. Figure 13a shows the mappings for positive peak pressure detection of the four ejection patterns while figure 13b shows the mappings for negative peak pressure detection of the four sweep patterns. These patterns as expected, show the ejection and sweep motion but differ significantly from those in figures 11 and 12 where the combined events in Groups I and II were retained. Clearly, the ejection and sweep motions are not exclusively distinct patterns within the organized motions, but coupled to form the spatially large organized structure.

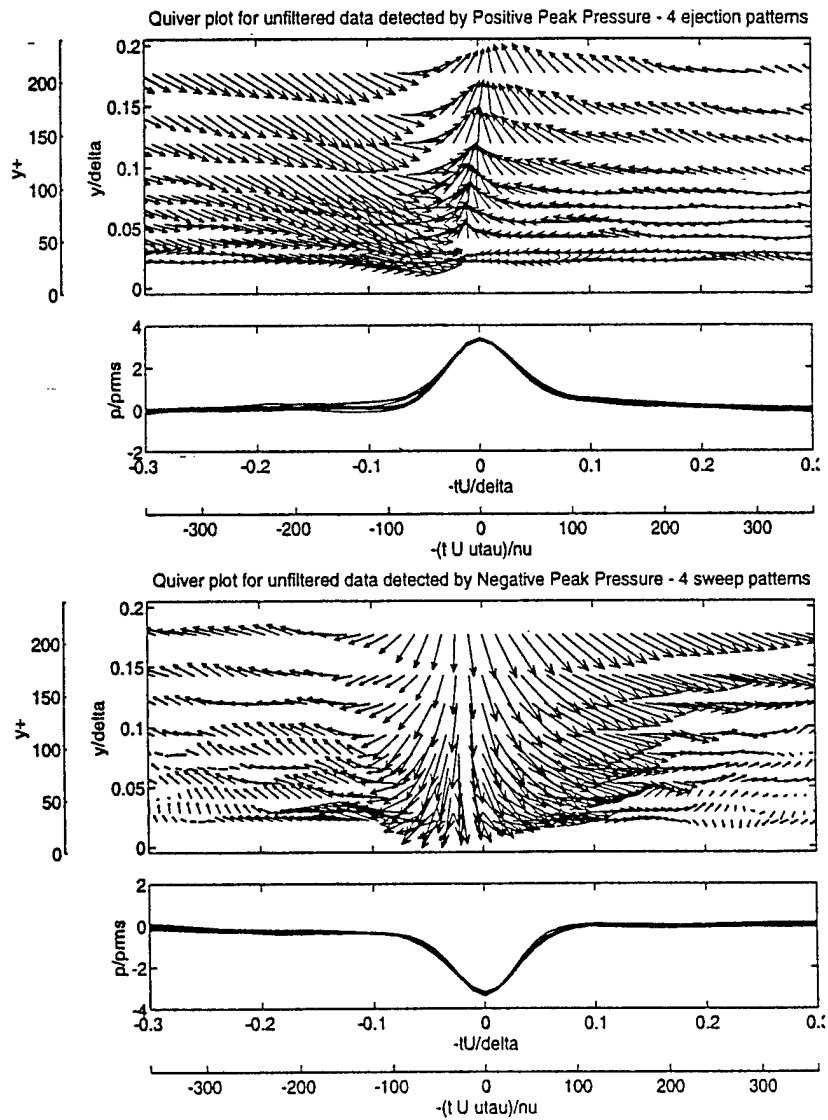


Fig. 13. Quiver plots showing the patterns associated with ejection (top) and sweep (bottom).

Chapter 4

Concluding Remarks and Future Work

These preliminary results using the TRAT algorithm developed by Nagano *et. al.* [4] are encouraging. They provided some new insight regarding the features of organized motions as observed from their wall pressure footprints.

The recognition of distinct near wall ejection and outer layer sweeps by the positive and negative pressure footprints is noteworthy. However, the clear delineation of these structures requires some form of filtering technique since the time and length scales of these structures are quite different. In previous work, Wavelet filtering did isolate the near-wall high frequency ejection process but probably distorted the large scale structures observed in the log-law region. The results of Kammeyer [1] based on LWPD cluster detection compared filtered and unfiltered data and showed some distinctions in the flow field. The results were inconclusive on the outer layer sweep motion.

Furthermore, the true nature of the pressure footprint contains both the high frequency near wall signatures reflected in positive pressure peaks, and the large scale sweep motions containing possibly lower frequency signatures with possibly negative peaks. How these combine to provide the total pressure signature is unresolved.

These issues are being addressed in the dissertation research of Russell [7]. In this research, an array of pressure transducers will be used to track the organized structures to learn more of their convective properties. In addition various filtering techniques (including TRAT) will be employed in an attempt to isolated and detect near wall active turbulent motions as well

as address the question of the coupling of these structures to large scale outer layer turbulent activity. By applying the bandpass filtering techniques to the data obtained from the array of transducers, it is expected that the "total" pressure signature will be more evident.

Acknowledgements

This work was supported by the Office of Naval Research with Dr. L. Patrick Purtell as scientific officer, under Grant # N00014-94-1-0011.

The data records used in this phase of the investigation were acquired by Dr. Mark Kammeyer. The authors are grateful for his cooperation.

Bibliography

- [1] Kammeyer, M., "An experimental investigation of organized turbulent motions and wall-pressure fluctuations in complex flows", Ph.D. Thesis, The Catholic University of America, December 1994
- [2] Penafiel, P., "Intermittent turbulence flow classification", 1995 (unpublished).
- [3] Wilczynski, V., "Organized Turbulent Structures and their Induced Wall Pressure Fluctuations", Ph.D. Thesis, The Catholic University of America, 1992.
- [4] Nagano, Y., Tagawa, M., "Coherent motions and heat transfer in a wall turbulent shear flow", *J. Fluid. Mech.*, 305: 127-157, 1995.
- [5] Casarella, M., Penafiel, M., Kammeyer, M., "Turbulence flow analysis using Wavelet filters", Report 2 ONR, 1995
- [6] Bogard, D. G., Tiederman, W. G., "Burst detection with single-point velocity measurements", *J. fluid Mech.*, 63: 389-413, 1986.
- [7] Russell, S., "Identification of Coherent Motions using Wall Pressure Signatures", Ph.D. thesis, The Catholic University of America, to be published.
- [8] Snarski, S. R., Lueptow, R. M., "Wall pressure and coherent Structures in a Turbulent boundary layer on a Cylinder in axial flow", *J. fluid Mech.*, 286: 137-171, 1995

Distribution List

Dr. Patrick Purtell
Office of Naval Research
S & T Division
800 North Quincy Street
Arlington VA 22217-5660

Dr. Spiro G. Lekoudis
Office of Naval Research
S & T Division
800 North Quincy Street
Arlington VA 22217-5660

Dr. Theodore M. Farabee
Carderock Division, Code 725
Naval Surface Warfare Center
Bethesda MD 20084

Dr. Richard M. Lueptow
Mechanical Engineering Dept.
Northwestern University
2145 Sheridan Road
Evanston IL 60208

Dr. William L. Keith
Code 2141
Naval Undersea Warfare Center
New London CT 06320

Dr. Candace E. Wark
Mech. & Aerospace Engr. Dept.
Illinois Inst. of Technology
10 West 32nd Street
Chicago IL 60616-3793

Dr. P. R. Bandyopadhyay
Weapons Tech/Undersea Systems
Naval Undersea Warfare Center
1176 Howell Street
Newport RI 02841-1708

Professor J. F. Morrison
Department of Aeronautics
Imperial College
Prince Consort Road
London, SW7 2BY UK

Professor Peter Bradshaw
Mechanical Engineering Dept.
Stanford University
Standord CA 94305-3030

Professor Ron F. Blackwelder
Aerospace Engineering Department
University of Southern California
Los Angeles CA 90089-1191

Dr. Vincent Wilczynski
U.S. Coast Guard Academy
15 Mohegan Avenue
New London CT 06320

Dr. Ronald Panton
Mechanical Engineering Dept.
University of Texas
Austin TX 78712

Professor R. Sreenivasan
Mason Laboratory
Yale University
New Haven CT 06520

Defence Technical (4 copies)
Information Center
Cameron Station
Alexandria VA 22304-6145

Dr. John Sullivan
Aerospace Science Lab
Purdue University
3 Purdue Airport
West Lafayette IN 47906-3371

Professor Dennis Bushnell
NASA-Langley Research Center
M/S 197
Hampton VA 23681

Professor John K. Eaton
Mechanical Engineering Dept.
Stanford University
Standord CA 94305-3030

Professor John Foss
Mechanical Engineering Dept.
Michigan State University
A-118 Research Complex - Engr.
East Lansing MI 48824

Dr. Mark Kammeyer
Code K24
NSWC
10901 New Hampshire Ave
Silver Spring MD 20903-5640